MW Journal of Science
ISSN: 3023-770X
https://doi.org/10.5281/zenodo.16745547 MW Journal of Science, 2025, 2, 2, 22-32

Antibacterial and Microstructural Evolution in Silver Modified NiTi Shape Memory Alloy

Berfin SAĞIR[1,2]*, Sevda KIRBAĞ[3], Yıldırım AYDOĞDU[4]

[1] Firat University, Faculty of Science, Department of Physics, Elazığ, TÜRKİYE
[2] Gazi University, Graduate School of Nature and Applied Sciences, Ankara, TÜRKİYE
[3] Firat University, Faculty of Science, Department of Biology, Elazığ, TÜRKİYE
[4] Gazi University, Faculty of Science, Department of Physics, Ankara, TÜRKİYE
*Corresponding author: bsagir@firat.edu.tr

Abstract

This study examines the microstructural properties, phase behavior, and antibacterial activity of nickel-titanium (NiTi) shape memory alloys (SMAs) doped with varying concentrations of silver (Ag). Five distinct alloys were produced through arc melting followed by homogenization. X-ray diffraction (XRD) analysis revealed that increasing Ag content stabilizes the B2 phase and suppresses martensitic transformation. Microstructural evaluations showed that low Ag content promoted grain refinement, whereas higher additions led to the formation of secondary phases. Disk diffusion tests indicated a notable antibacterial effect in the Ag4 sample, particularly against Escherichia coli (E. coli) and Staphylococcus aureus (S. aureus). The results suggest that Ag doping enhances the antimicrobial efficacy of NiTi alloys, making them promising candidates for reducing infection risks in biomedical applications.

Keywords: NiTiAg alloy, antibacterial, shape memory alloys

Introduction

Shape memory alloys (SMAs) are a class of intelligent materials that exhibit a unique property known as the shape memory effect (SME). This phenomenon enables SMAs to regain their original shape after undergoing significant deformation at a temperature below a specific threshold, upon exposure to external stimuli such as heat, electric current, or a magnetic field. The SME allows these alloys to be trained to recall different shapes at various temperatures, resulting in a wide range of applications in fields including biomedical engineering, aerospace technology, soft robotics, civil engineering, and actuators. Furthermore, SMAs display superelasticity (SE), characterized by large elastic elongation (up to 8%) and pseudoelastic recovery (up to 15%) when stimulated beyond a certain transition temperature, which solidifies their classification as smart materials [1-3]. The high-temperature austenite phase, which exhibits a body-centered cubic (BCC) crystal structure, undergoes a transformation into a distorted monoclinic martensite structure upon cooling below a specific transformation temperature [4]. The behavior exhibited by shape memory alloys (SMAs) is primarily attributed to their reversible phase transformation between the martensite and austenite phases, which can be triggered by thermal or mechanical stimuli. This transformation enables SMAs to recover their original structure after deformation [5]. Shape Memory Alloys (SMAs) display a unique characteristic known as pseudoelasticity or superelasticity, which distinguishes them from conventional elastic metals. Unlike true elasticity in bulk metals, which arises from variations in interatomic spacing governed by Hooke's law, superelasticity in

SMAs is a result of stress-induced phase transformations. The material exhibits elastic behavior, returning to its original shape upon removal of the applied load without any residual deformation [6, 7].

Nickel-titanium (NiTi) shape memory alloys are the most commonly utilised shape memory alloys, typically consisting of nearly equiatomic concentrations of nickel and titanium [4]. These alloys display several advantageous properties, including SME, superelasticity, biocompatibility, and osseointegration. The SME can be categorised into one-way and two-way varieties. Significant changes in the mechanical properties of the alloy, including stiffness, yield strength, and electrical resistivity, occur mainly due to modifications in electron bonding during cooling through a critical transformation temperature range [8].

Most research on internal friction in SMAs has centred on pinpointing the frictional peaks that occur during heating and cooling cycles. The damping ability of SMAs, especially those with a stable martensitic microstructure, is crucial in applications needing energy absorption. Limited research currently exists on the connection between damping ability and other properties of shape memory alloy, yet a close relationship is expected due to the mobility of martensite interfaces [9]. The distinct mechanical and chemical properties of NiTi alloys have contributed to their widespread use in minimally invasive surgical procedures, orthodontics, and orthopedic implantation. Their ability to undergo reversible phase transformations, combined with good corrosion resistance, biocompatibility, low cytotoxicity, and significant strength and ductility, makes them suitable for biomedical applications [10].

The poor antibacterial properties of NiTi alloys present a significant limitation in biomedical applications, where bacterial infections associated with implants can lead to severe complications, including implant failure, prolonged hospitalization, and the need for revision surgeries. To address these risks, researchers have focused on incorporating antibacterial agents into implant materials, with silver (Ag) emerging as a key candidate due to its broad-spectrum antibacterial activity and relatively low cytotoxicity. Silver's antimicrobial effect is achieved through the disruption of bacterial membranes and inhibition of essential enzymatic processes [11, 12]. Silver (Ag) has been extensively researched in recent years for its potential to enhance the antibacterial properties of various base metals. Furthermore, it has been widely utilised to prevent wound infections [13, 14]. Incorporation of silver into NiTi alloys is anticipated to enhance not only their antibacterial efficacy but also their thermomechanical and microstructural properties. Consequently, NiTiAg composites are regarded as promising candidates for achieving superior mechanical performance and increased infection resistance relative to conventional NiTi alloys [15].The concentration and distribution of silver within the NiTi matrix are crucial factors in determining its overall performance. Although the addition of silver can enhance mechanical strength, corrosion resistance, and biocompatibility, it may also result in compromises such as phase instability or mechanical degradation if not optimised correctly. Research has demonstrated that surface films containing 4-10 at.% Ag can provide a favourable balance of these properties, making them promising candidates for advanced medical implant applications [16].

This research offers insight into the practicality and constraints of incorporating silver (Ag) into nickel-titanium (NiTi) systems for biomedical purposes through the application of systematic alloying techniques and advanced characterisation methods.

Experimental

High purity (99.9%) powdered Ni, Ti and Ag components were used in this study. 25 grams of each alloy were formed and powder mixtures were made using the atomic percentages listed in the Table 1. The

following equation was used to determine the mass fraction of each element in the alloys based on the atomic percentages of the elements:

$$\%wt.Ni = \%at.\frac{m_{ANi}}{\%at.m_{ANi} + \%at.m_{ATi} + \%at.mA_{Ag}}\ x\ 100$$

When selecting the alloy ratios for this study, the nickel content of the NiTiAg alloys remained constant, while the titanium percentage was reduced and the silver content was increased. These powder combinations were shaped into 13 mm diameter pellets ready for melting.

Table 1. Atomic and mass percentages of NiTiAg alloys

Sample	Atomic Percentage			Mass Percentage			
Elements	Ni	Ti	Ag	Ni	Ti	Ag	e/a
Ag_0	51	49	0	56.061	43.939	0	7.06
Ag_1	51	48	1	55.438	42.564	1.998	7.03
Ag_2	51	47	2	54.829	41.219	3.952	7.00
Ag_3	51	46	3	54.233	39.904	5.862	6.97
Ag_4	51	45	4	53.650	38.617	7.733	6.94

Arc melting was used to form pelletised NiTiAg shape memory alloys. To homogenise the alloys in the system, the melting procedure was repeated many times while the samples were in the system. After fabrication, the alloys were produced in bulk. The bulk alloys underwent a second homogenisation process of 900 °C 24 h in a muffle furnace. Differential Scanning Calorimetry (DSC) is was used determine phase transformaiton of produced NiTiAg alloy with 10 °C/min. heating and cooling rate in nitrogen atmosphere. Crystal structure of NiTiAg alloys were detected by using X ray diffractometer. Microstructure image of alloys were taken with a Nikon Eclipce LV100ND industrial microscope at room temperature connected to the microscope. Before the image was taken, all samples were embedded in polyester resin and prepared for polishing. Then, the polishing process was carried out and made ready for etching. In the etching process, 4HNO3+1HF+5H2O solution was prepared for NiTiAg alloys. The samples were kept in the prepared solution for 30 seconds and etching process was carried out. Standard antibiotic discs, *E. coli* ATCC 25922 and *S. aureus* COWAN 1 microorganisms were used as controls of the study. Antibacterial effect is evaluated using the disc diffusion method [3]. This procedure involves inoculation of bacterial strains into the medium followed by incubation at 35±1 °C for 24 hours. Cultures grown in medium were transferred to broth tubes following MacFarland (0.5) standard for turbidity adjustment. After sterilisation in an Erlen and cooling to 45-50 °C, the cultures in the medium were injected c/o1 (106 bacteria/ml) onto "Muller Hinton Agar". After intensive mixing, 9 cm diameter sterile petri dishes were filled with 15 ml each to ensure homogenous distribution. Petri dishes prepared in this way were kept at 4 °C for 1.5-2 hours and then inoculation plates were incubated at 37±0.1 °C for 24 hours. At the end of the given time, inhibition zones were measured in millimetres.

Results and Discussion

Figure 1. shows the heat flux curves of NiTi binary alloy and increasingly Ag doped alloys in the range from -50 ℃ to 250 ℃ in a nitrogen gas atmosphere with a heating-cooling rate of 10 ℃/min.

Austenite→martensite, martensite→austenite phase transformation was not observed in any of these curves. This result is expected. Therefore, martensitic phase transformation has been completed before at -50 ℃.

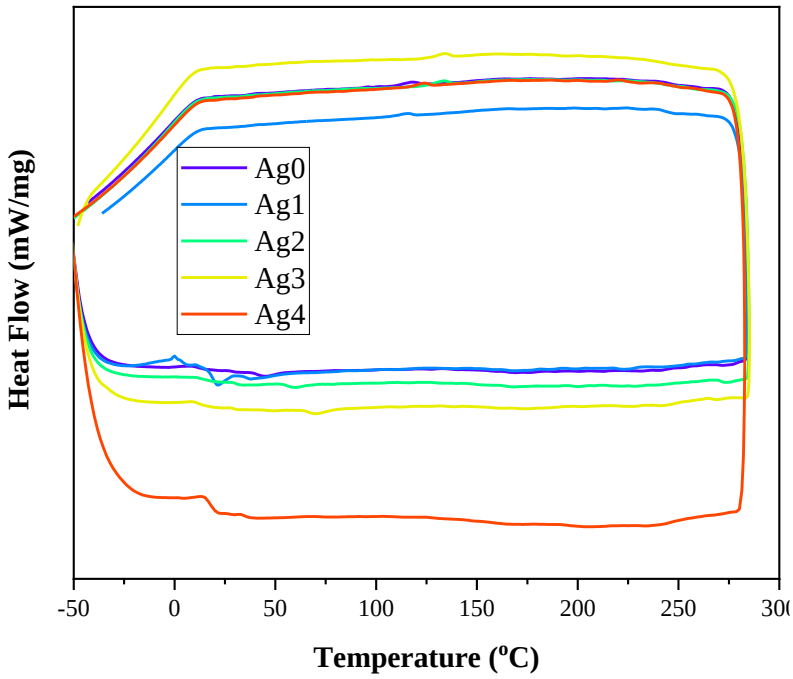

Figure 1. Temperature-varying heat flux curve of NiTiAg alloys (The alloys are named Ag0, Ag1, Ag2, Ag3, Ag4 and Ag5 according to their silver content)

Figure 2 shows the X-ray diffraction patterns (XRD) of NiTiAg alloys containing different amounts of silver (Ag). The samples are named Ag0, Ag1, Ag2, Ag3 and Ag4 according to the increasing Ag content. Characteristic peaks of two main phases were detected in the XRD patterns: the high-temperature phase B2 (NiTi) phase (denoted by *) and the low-temperature martensitic phase B19' (NiTi) phase (denoted by ◆). According to the X-ray curves, it is concluded that the phase composition is significantly affected by the increase in Ag content. The existence of the B2-NiTi phase corresponding to planes (110) and (211) is confirmed by the sharp peaks seen at 2θ ≈ 42.8° and 78.2° in the Ag-free NiTi sample. This result is consistent with the B2 (austenite) phase described in the literature by Qader et al. (2022) and Gao et al. (2024) [17, 18]. It is clearly seen that the diffraction peaks of the B2 phase are dominant in all samples. This shows that the B2 phase forms the basic crystal structure in the samples and that the stability of this phase is maintained, especially with increasing Ag content. The peaks belonging to the B19' phase were observed weakly only in Ag0, Ag1, Ag2 and Ag3 samples, and it is considered that this phase is present in low proportions or partially formed due to the stress-cooling effect due to heat treatment. It is seen that with the increase in Ag doping, the B19' phase is completely suppressed and the structure is completely stabilized in the B2 phase. This finding indicates that the Ag element plays a role in increasing the B2 phase stability in the NiTi matrix. This is also supported in the literature. For example, studies such as Kim et al. (2004) and Liu et al. (2011) have shown that third element additives (especially elements such as Cr, Co, Mn) increase the stability of the B2 phase, lower the transformation temperatures and prevent martensitic transformation at room temperature [19, 20]. In conclusion, XRD results show that the increased Ag content stabilizes the B2 phase and prevents the formation of the B19' martensitic phase.

This provides an important structural advantage in controlling the thermomechanical behavior of Ag-doped NiTi alloys.

Debye Scherrer's equation, which depends on some parameters including width at half maximum (FWHM), Bragg angle (θ), wavelength, was used to calculate the crystal sizes obtained from XRD data. The crystal size (D) of the alloys was determined using the Scherrer equation. The Scherrer equation was used to determine the crystal size of each alloy depending on the wavelength of the X-ray source (λKα(Cu)) [21].

$$D = K\,(\lambda / B\cos\theta)$$

Here, the FWHM is denoted by B. for XRD experiments, the shape factor K = 0.9 and the wavelength λ was chosen at 1.5406 Å. The Ag doping did not show a significant change in the crystal size, but fluctuated. This value is in the range of 1.0-1.5 nm.

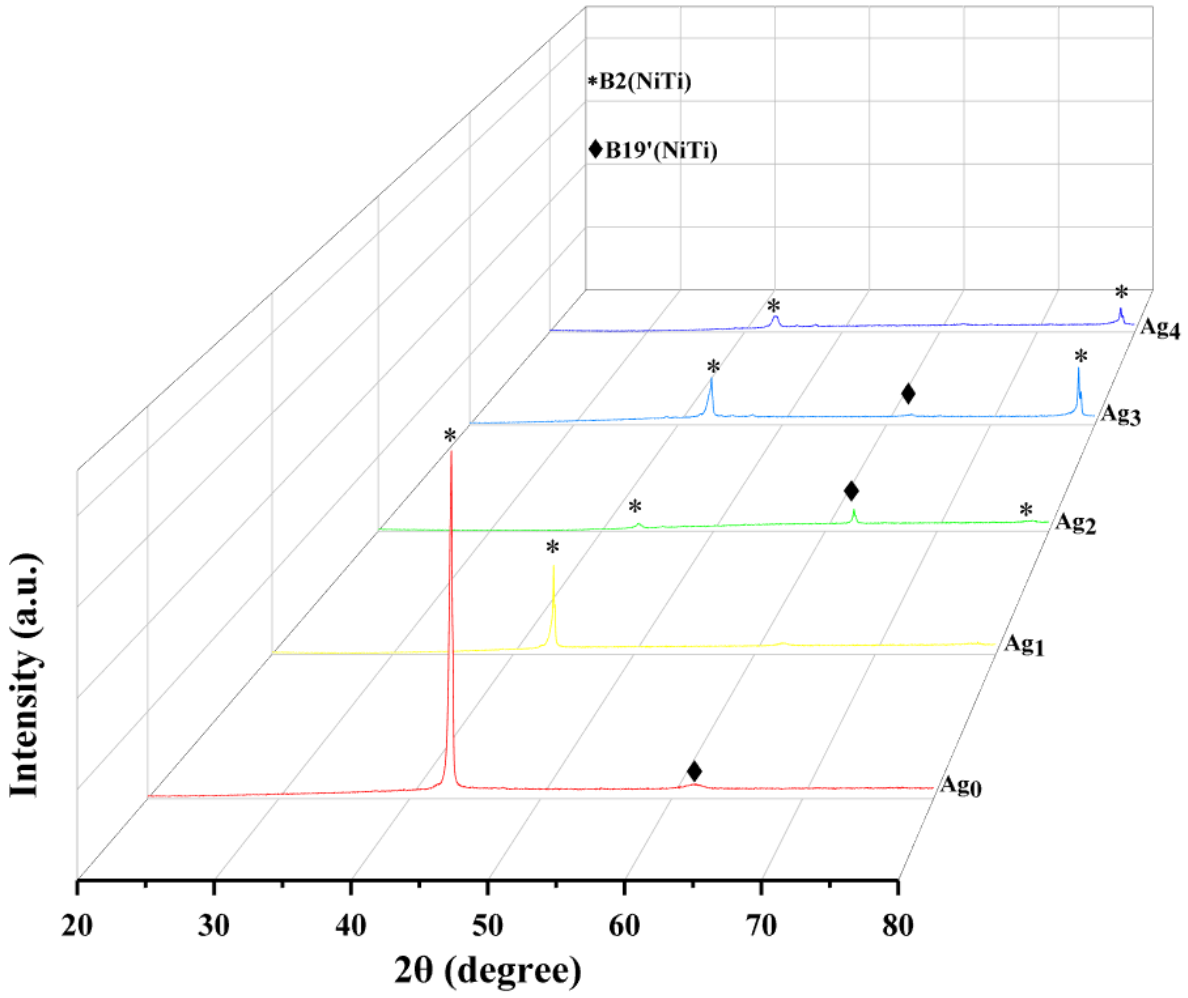

Figure 2. XRD diffractograms of NiTiAg alloys (The alloys are named Ag0, Ag1, Ag2, Ag3, Ag4 and Ag5 according to their silver content)

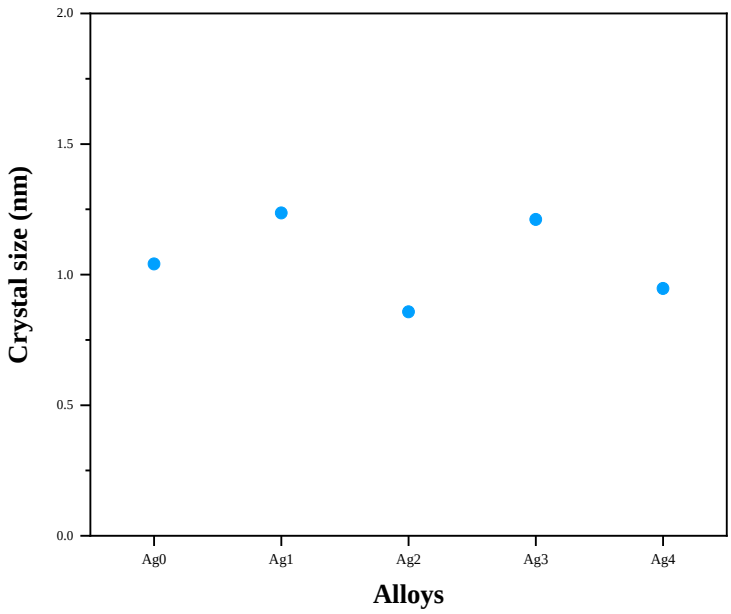

Figure 3. Crystal dimensions of NiTiAg alloys (The alloys are named Ag0, Ag1, Ag2, Ag3, Ag4 and Ag5 according to their silver content)

The reference Ag0 sample exhibited a homogeneous and coarse-grained structure due to the absence of silver and no second phase formation or microstructural distortion was observed (Figure 4). This is consistent with the characteristic structure of binary NiTi alloys reported in the literature [22]. The low percentage of Ag doping (Ag1) caused a significant reduction in grain size, indicating that Ag enhances heterogeneous nucleation due to its limited solubility. Zhang et al. (2012) emphasized the effect of low Ag doping to improve structural homogeneity [23]. In the Ag2 sample, second phase formations and distinct grain boundaries were observed and further refinement of the precipitate size was detected. Such phases are thought to be TiNi or Ag-rich intermetallic compounds. It has been reported in the literature that Ag doping can cause the formation of such secondary phases and this can affect the mechanical properties and transformation behavior properties [24]. In the Ag_3 sample where the Ag content was increased to 3%, optical micrographs revealed prominent precipitates and phase separations, indicating that the Ag solubility in the matrix was exceeded. Baigonakova et al. (2020) reported that Ag additives in excess of 2% lead to the formation of Ti_2(Ni,Ag)-like intermetallic phases that disrupt microstructural homogeneity [16].

Standard antibiotic discs were used as controls for the studies of *E. coli* ATCC 25922 and *S. aureus* COWAN 1 microorganisms. Bacterial strains were inoculated into the medium and then incubated at 35±1 °C for 24 hours. The cultures grown in the medium were transferred to broth tubes following the MacFarland (0.5) standard for turbidity adjustment. After sterilisation in an Erlen and cooling to 45-50 °C, the cultures in the medium were injected into 'Muller Hinton Agar' c/o1 (106 bacteria/ml). After intensive mixing, 9 cm diameter sterile petri dishes were filled with 15 ml of bacteria each to ensure homogeneous distribution. The petri dishes prepared in this way were kept at 4 °C for 1.5-2 hours, then the inoculation plates were incubated at 37±0.1 °C for 24 hours and the inhibition zones were measured in millimetres at the end of the given time. For NiTiAg alloys, Ni, Ti, Ag pure elements were evaluated separately and inhibition zones were measured against both bacterial species (Figure 5). The sizes of the zones resulting from antibacterial tests of Ni, Ti, Ag pure elements are shown in the Table 2. Both bacterial species were moderately inhibited by silver (<2->2 mm). Ni showed antibacterial properties at 2 mm, while Ti did not

show antibacterial properties. These components are not as effective as normal antibiotic discs (10 mm and 8 mm).

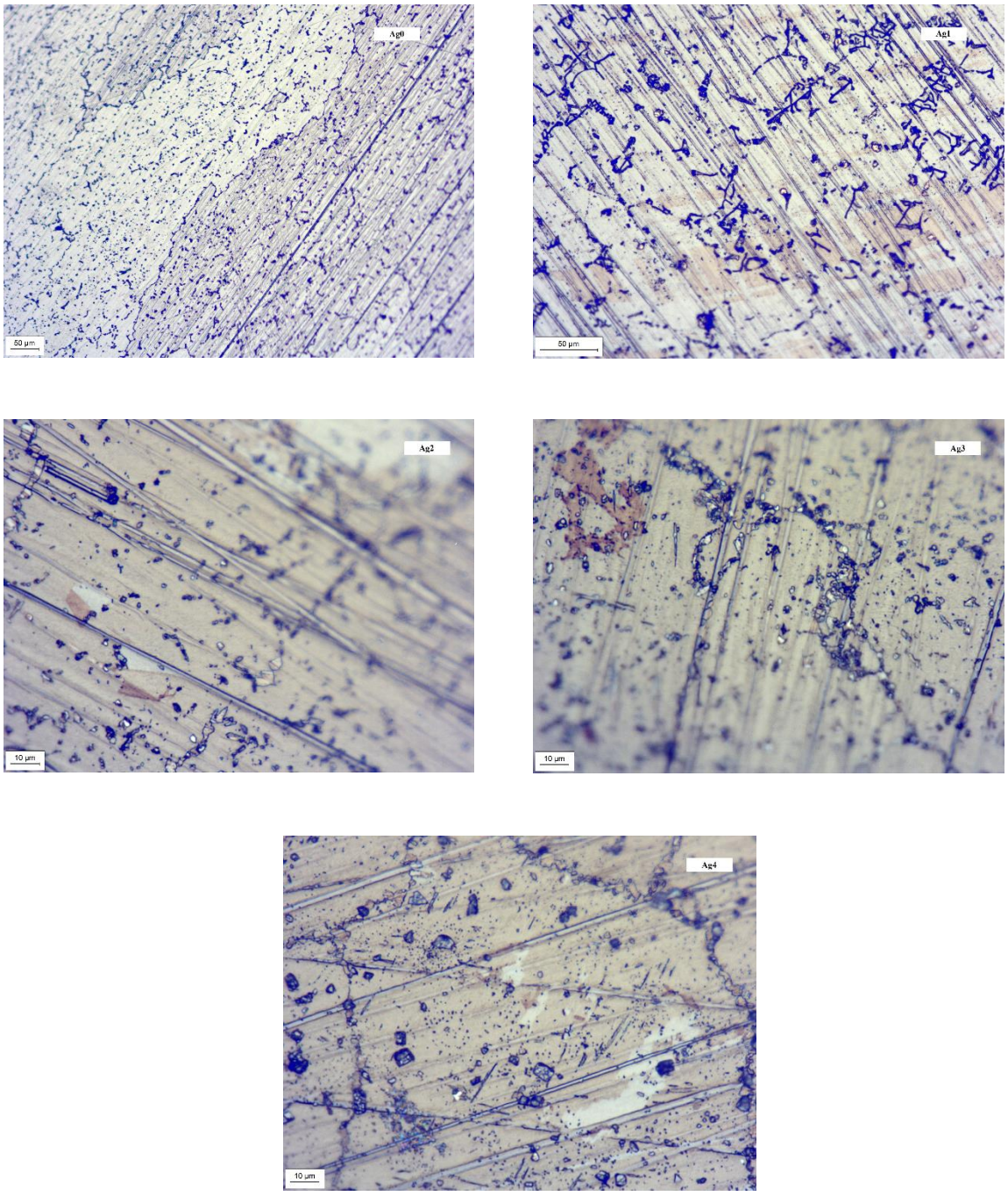

Figure 4. Metallographic images of NiTiAg alloys

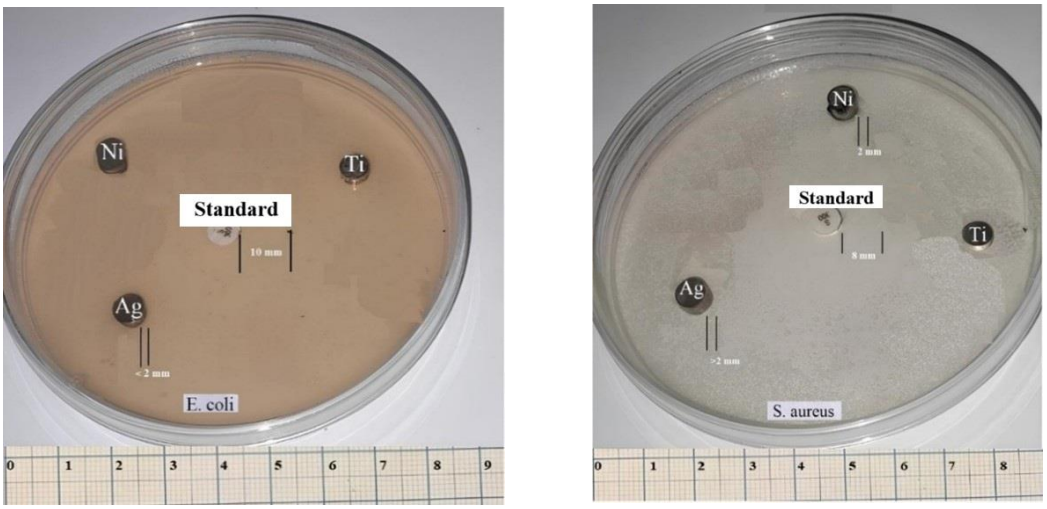

Figure 5. Antibacterial zones of pure metals (Ni, Ti, Ag)

Table 2. Antibacterial zones of pure metals (Ni, Ti, Ag)

Sample	*E. coli* (mm)	*S. aureus* (mm)
Ni	-	2
Ti	-	-
Ag	< 2	> 2
Standard	10	8

The Ag4 sample exhibited the strongest antibacterial activity, with inhibition zones of 2 mm against *Staphylococcus aureus (S. aureus)* and 3 mm against *Escherichia coli (E. coli)* (Figure 6). Notably, samples with low silver concentrations, such as Ag0 and Ag1, demonstrated no inhibition against *E. coli*, but did exhibit a low level of inhibition against S. aureus, exceeding 1 mm. In comparison, all alloy samples displayed weak antibacterial activity, with inhibition zones of less than 9 mm for *E. coli* and less than 11 mm for *S. aureus*. However, as the silver doping concentration increased, the antibacterial activity of the alloys significantly improved (Table 3). These findings suggest that incorporating silver into NiTi alloys may be a viable strategy to enhance their antibacterial properties. The results are consistent with research indicating that silver ions inhibit bacterial function by disrupting proteins and enzymes in the cell membrane [11, 12].

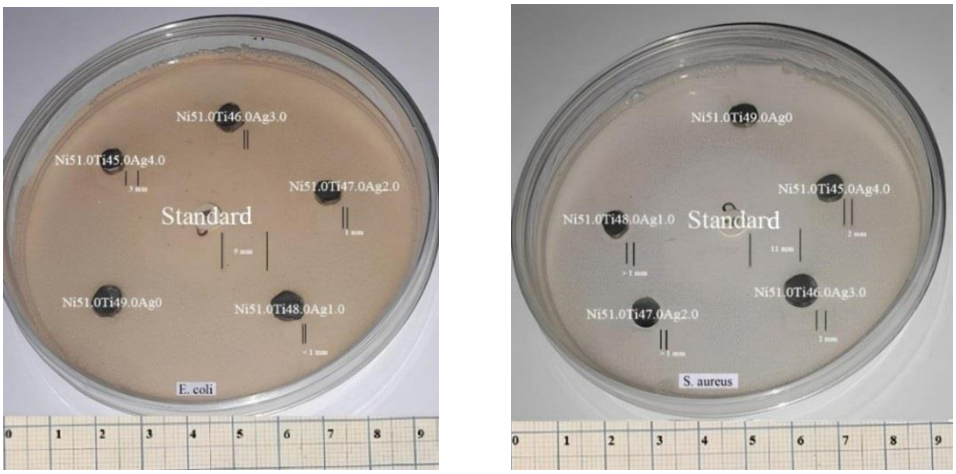

Figure 6. Antibacterial zones of NiTiAg alloys

Table 3. Antibacterial zones of NiTiAg alloys

Sample	*E. coli* (mm)	*S. aureus* (mm)
Ag_0	-	-
Ag_1	-	> 1
Ag_2	1	> 1
Ag_3	1	2
Ag_4	3	2
Standard	9	11

Conclusion:

This study successfully fabricated and characterised NiTi-based shape memory alloys with varying silver (Ag) content in terms of structural, thermal, and antibacterial properties. The results showed that increasing Ag content significantly affected the phase composition and microstructure of the alloys. X-ray diffraction analysis confirmed the stabilisation of the B2 phase and suppression of the martensitic B19' phase with higher Ag concentrations. Optical microscopy demonstrated that low Ag doping led to grain refinement, whereas higher doping levels resulted in secondary phase formation and microstructural heterogeneity. Antibacterial testing via the disc diffusion method showed that Ag incorporation enhanced the antimicrobial properties of the alloys, with the Ag4 sample exhibiting the largest inhibition zones against *E. coli* and *S. aureus*. While the overall antibacterial performance remained moderate compared to standard antibiotic controls, a positive correlation between Ag content and antibacterial effectiveness was observed. Although no clear martensitic transformation was detected in differential scanning calorimetry analysis, likely due to the suppressive effect of Ag on transformation temperatures, the alloys still present considerable potential for biomedical use. Specifically, their improved antibacterial performance and structural stability make them promising materials for temporary implant systems and antibacterial surface applications.

Acknowledgements:

This article is a part of Master thesis (The Production of Shape Memory Alloys and Investigation of Antibacterial Properties for Biomedical Applications, June 2025) study of Berfin SAĞIR.

References:

[1] Bhardwaj, A., et al., Characterization of mechanical and microstructural properties of constrained groove pressed nitinol shape memory alloy for biomedical applications. Materials Science and Engineering: C, 2019. **102**: p. 730-742.

[2] Chaudhary, K., V.K. Haribhakta, and P.V. Jadhav, *A review of shape memory alloys in MEMS devices and biomedical applications.* Materials Today: Proceedings, 2024.

[3] Shukla, U. and K. Garg, Journey of smart material from composite to shape memory alloy (SMA), characterization and their applications-A review. Smart Materials in Medicine, 2023. **4**: p. 227-242.

[4] Es-Souni, M., M. Es-Souni, and H. Fischer-Brandies, *Assessing the biocompatibility of NiTi shape memory alloys used for medical applications.* Analytical and bioanalytical chemistry, 2005. **381**: p. 557-567.

[5] Jiao, Z., et al., Phase transition, twinning, and spall damage of NiTi shape memory alloys under shock loading. Materials Science and Engineering: A, 2023. **869**: p. 144775.

[6] Han, X., S. Mao, and Z. Zhang, *Superelasticity and the Shape Memory Effect*, in *Encyclopedia of Nanotechnology*, B. Bhushan, Editor. 2016, Springer Netherlands: Dordrecht. p. 3874-3880.

[7] Nargatti, K. and S. Ahankari, Advances in enhancing structural and functional fatigue resistance of superelastic NiTi shape memory alloy: A Review. Journal of Intelligent Material Systems and Structures, 2022. **33**(4): p. 503-531.

[8] Patel, S.K., et al., A review on NiTi alloys for biomedical applications and their biocompatibility. Materials today: proceedings, 2020. **33**: p. 5548-5551.

[9] Liu, Y., et al., *Some aspects of the properties of NiTi shape memory alloy.* Journal of alloys and compounds, 1997. **247**(1-2): p. 115-121.

[10] Keun-Taek Oh 1, U.-H.J., Gee-Ho Park, Chung-Ju Hwang, Kyoung-Nam Kim, *Effect of silver addition on the properties of nickel-titanium alloys for dental application.* Journal of biomedical materials research Part B, 2006. **76**(2): p. 306–314.

[11] Lansdown, A., *Silver in health care: antimicrobial effects and safety in use.* CURRENT PROBLEMS IN DERMATOLOGY-BASEL-, 2006. **33**(R): p. 17.

[12] Rai, M., A. Yadav, and A. Gade, *Silver nanoparticles as a new generation of antimicrobials.* Biotechnology advances, 2009. **27**(1): p. 76-83.

[13] Zhang, E., et al., *Antibacterial metals and alloys for potential biomedical implants.* Bioactive materials, 2021. **6**(8): p. 2569-2612.

[14] Jiao, J., et al., *Recent advances in research on antibacterial metals and alloys as implant materials.* Frontiers in cellular and infection microbiology, 2021. **11**: p. 693939.

[15] Salman, K.D., et al., Microstructural Analysis and Mechanical Characterization of Shape Memory Alloy Ni-Ti-Ag Synthesized by Casting Route. Applied Sciences, 2022. **12**(9): p. 4639.

[16] Baigonakova, G., et al., Influence of silver addition on structure, martensite transformations and mechanical properties of TiNi–Ag alloy wires for biomedical application. Materials, 2020. **13**(21): p. 4721.

[17] Qader, I.N., E. Ercan, and A. Orhan, Effect of boron element additions on microstructure, biocompatibility, and thermodynamic parameters of NiTi shape memory alloy. JOM, 2022. **74**(11): p. 4402-4409.

[18] Gao, J., et al., Well-Adhered Ti Alloying Layer on NiTi Alloy: Surface Ni Content, Corrosion Resistance, and Cytocompatibility. Journal of Materials Engineering and Performance, 2024: p. 1-11.

[19] Kök, M. and G. Ateş, The effect of addition of various elements on properties of NiTi-based shape memory alloys for biomedical application. The European Physical Journal Plus, 2017. **132**(4): p. 185.

[20] Kök, M., et al., The effects of cobalt elements addition on Ti2Ni phases, thermodynamics parameters, crystal structure and transformation temperature of NiTi shape memory alloys. The European Physical Journal Plus, 2019. **134**(5): p. 197.

[21] Kök, M., et al., Thermal stability and some thermodynamics analysis of heat treated quaternary CuAlNiTa shape memory alloy. Materials Research Express, 2019. **7**(1): p. 015702.

[22] Waitz, T., et al., Size-dependent martensitic transformation path causing atomic-scale twinning of nanocrystalline NiTi shape memory alloys. Europhysics Letters, 2005. **71**(1): p. 98.

[23] Zhang, H., et al., Influence of Ag on microstructure, mechanical properties and tribological properties of as-cast Al-33Zn-2Cu high-zinc aluminum alloy. Journal of Alloys and Compounds, 2022. **922**: p. 166157.